tropopause temperatures associated with a troposphere greenhouse effect, would also be important. □

Received 11 October 1988; accepted 13 March 1989.

1. Crutzen, P. & Arnold, F. *Nature* **324,** 651–655 (1986).
2. Toon, O. B., Hamill, P., Turco, R. P. & Pinto *Geophys. Res. Lett.* **13,** 1284 (1986).
3. McElroy, M. B., Salawitch, R. J. & Wofsy, S. C. *Geophys. Res. Lett.* **13,** 1296–1299 (1986).
4. Poole, L. R. & McCormick, M. P. *Geophys. Res. Lett.* **15,** 21–23 (1988).
5. Molina, M. J., Tso, T. L., Molina, L. T. & Wang, F. C. Y. *Science* **238,** 1253–1257 (1987).
6. Tolbert, M. A., Rossi, M. J., Malhorta, R. & Golden, D. *Science* **238,** 1258–1260 (1987).
7. Leu, M. T. *Geophys. Res. Lett.* **15,** 17–20 (1988).
8. Hanson, D. & Mauersberger, K. *Geophys. Res. Lett.* **15,** 855–858 (1988).
9. Arnold, F., Heitmann, H. & Oberfrank, K. *Planet. Space Sci.* **32,** 1567–1576 (1984).
10. Arnold, F. & Hauck, G. *Nature* **315,** 307–309 (1985).
11. Knop, G. & Arnold, F. *Planet. Space Sci.* **33,** 983–986 (1985).
12. Arnold, F., Knop, G. & Ziereis, H. *Nature* **321,** 505–507 (1986).
13. Knop, G. & Arnold, F. *Planet. Space Sci.* **35,** 259–266 (1987).
14. Arnold, F. & Knop, G. *Int. J. Mass Spectrom. Ion Proc.* **81,** 33–44 (1987).
15. Knop, G. & Arnold, F. *Geophys. Res. Lett.* **14,** 1262–1265 (1987).
16. Arnold, F. *et al. A. Rep. Max-Planck-Institut für Kernphysik* (1988).
17. Gille, J. C. *et al. J. geophys. Res.* **89,** 5179–5190 (1984).
18. Gille, J. C. & Russell III, J. M. *J. geophys. Res.* **89,** 5125–5140 (1984).
19. Austin, J., Garcia, R. R., Russell, J. M., Solomon, S. & Tuck, A. F. *J. Geophys. Res.* **91,** 5477–5485 (1986).
20. Jackman, C. H., Guthrie, P. D. & Kaye, J. A. *J. geophys. Res.* **92,** 995–1008 (1987).
21. Girard, A., Gramont, L., Loisnard, N., Boiteux, S. & Fergant, G. *Geophys. Res. Lett.* **9,** 135–138 (1982).
22. Girard, A. *et al. J. geophys. Res.* **88,** 5377–5392 (1983).
23. Murcray, D. G., Barker, D. B., Brooks, J. N., Goldman, A. & Williams, W. J. *Geophys. Res. Lett.* **2,** 223–225 (1975).
24. Poole, L. R., Osborn, M. T. & Hunt, W. H. *Geophys. Res. Lett.* **15,** 867–870 (1988).
25. *Atmospheric Ozone 1985, WMO Report* No. 16, Vol. II, 474 (1985).
26. US Standard Atmosphere, 1966. U.S. Government Printing Office, Washington D.C. 20402.
27. Kiehl, J. T., Boville, B. A. & Priegleb, B. P. *Nature* **332,** 501–504 (1988).

ACKNOWLEDGEMENTS. The authors are grateful to the many colleagues who participated in the CHEOPS expeditions and contributed to the success of this project. In particular, we acknowledge support from Esrange, CNES and DFVLR, and the collaboration with KFA Jülich, DFVLR, NASA. We are grateful to the team of the Meteorological Institute of the Free University of Berlin, especially K. Labitzke, K. Paetzold, B. Naujokat and R. Lenchow, who provided us with essential information and predictions on stratospheric meteorology. We also thank the technical staff of the MPIK, particularly K. Bechberger, W. Dann, B. Preissler, H. Sauer and W. Thron. This project was funded bythe BMFT through GSF.

Increased particle flux to the deep ocean related to monsoons

R. R. Nair*, V. Ittekkot†, S. J. Manganini‡, V. Ramaswamy*, B. Haake†, E. T. Degens†, B. N. Desai* & S. Honjo‡

* National Institute of Oceanography, Dona Paula, Goa-403004, India
† Geologisch-Paläontologisches Institut und Museum, Universität Hamburg, Bundesstrasse 55, D-2000 Hamburg 13, FRG
‡ Woods Hole Oceanographic Institution, Woods Hole, Massachusetts 02543, USA

MONSOONS cause seasonal reversals in the surface circulation of the northern Indian Ocean[1]. In the Arabian Sea this results in the upwelling of nutrient-rich water along the coasts[2–4], making it one of the highly productive regions of the world's oceans. To assess the impact of monsoon-driven processes on the downward particle flux variations in the open ocean we deployed three moored arrays consisting of six time-series sediment traps at selected locations in the western, central and eastern parts of the deep northern Arabian Sea. Strong seasonality was recorded in particle flux at all three sites with peaks during the south-west and north-east monsoons. High primary productivity during the monsoons resulting from wind-induced mixed-layer deepening and the associated nutrient injection to the euphotic zone appeared to be the main factor controlling the observed particle flux pattern. These findings may shed light on CO_2 uptake during glaciation when wind speeds were higher.

Three mooring systems, each consisting of two time-series sediment traps[5]—one 1,000 m below the sea surface and the other 1,000 m above the sea bottom—were deployed at three sites in the western, central and eastern Arabian Sea (Fig. 1). The collecting cups were poisoned with mercuric chloride before deployment. The sediment traps were programmed to measure the flux of sinking particles at intervals of 12 to 13 days each over a duration of six months per deployment. They have been recovered and redeployed three times since May 1986 using the research vessels RV *Sonne* and the ORV *Sagar Kanya*. Here we report the results obtained during the first year of deployment.

On recovery of the traps, the samples were wet-sieved and split using a precision rotary splitter. One quarter of the <1 mm size fraction was filtered through pre-weighed Nuclepore filters (0.5 μm) and dried at 40 °C. This fraction was used for flux calculations and for analysis of first order parameters such as carbonate, opal, lithogenic, organic carbon, and nitrogen[6,7].

At all three sites the flux of sinking particles showed seasonality which is strongly related to the monsoons with higher fluxes during the south-west (June to September) and north-east (December to February) monsoons (Fig. 2). Individual fluxes differed by more than two orders of magnitude. Differences between maximum and minimum fluxes during these two periods were highest at the western and eastern sites; these are characterized by their proximity to the upwelling centres along the Somali and the Arabian coasts and the Indian continental shelf, respectively. The similarity in flux patterns not only at sites close to the upwelling centres, but also at the site in the central Arabian sea, indicates that factors other than coastal upwelling might also be responsible for the higher particle fluxes. The close relationship observed between particle fluxes and wind speeds at the three sites provides a clue (Fig. 3). Higher wind speeds lead to a deepening of the mixed layer and the introduction of nutrient-rich subsurface waters into the euphotic zone[8,9]. Mixed-layer deepening from 30 to 40 m during the pre-monsoon period to more than 100 m during the south-west monsoon have been reported[10]. The wind-induced nutrient pumping into the euphotic zone is especially effective in the Arabian Sea as subsurface waters are extremely rich in nutrients[11]. This results in high primary production during both monsoons[12–14] and this high 'new production' is reflected in high particle fluxes to the deep sea. An exception to this is the eastern Arabian Sea during the north-east monsoon. Here particle fluxes are extremely low, although wind speeds are only slightly lower than at the other stations. This could be due to the absence of regular winter blooms caused by the inflow of low-salinity water from the eastern tropical Indian Ocean, which leads to stronger stratification and to lower productivity[13].

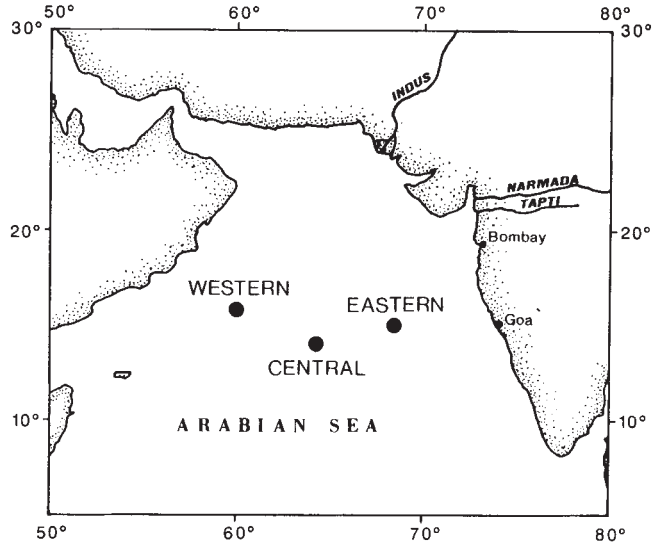

FIG. 1 Locations of mooring systems in the western, central and eastern Arabian Sea. The distance of the moorings from the nearest coast are 520, 930 and 430 km for the eastern, central and western trap, respectively.

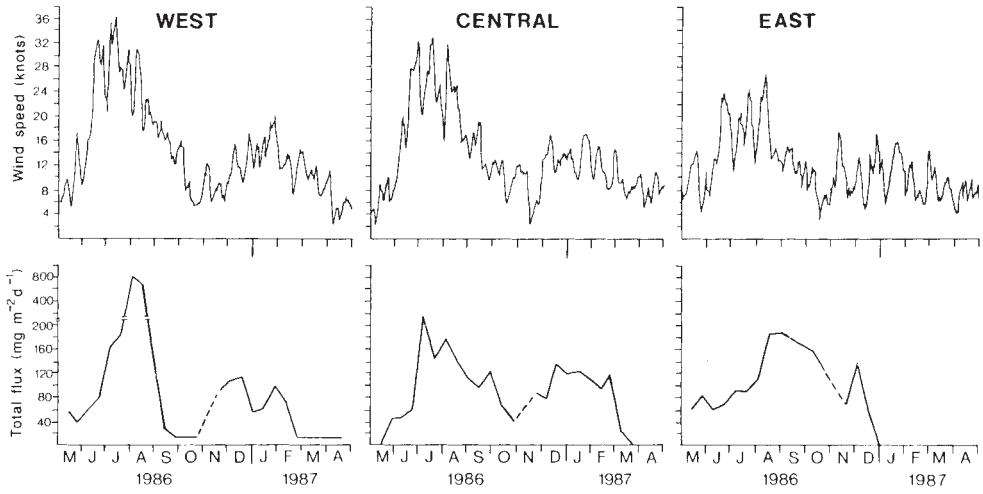

FIG. 2 Seasonal variations of particle fluxes to the deep Arabian Sea (bottom) from time-series sediment trap deployments (sampling intervals 12–13 days) at the western, central and eastern Arabian Sea (trap depths: 3,020 m, 2,900 m and 2,770 m, respectively), and wind-speed data during the period of deployment (top) compiled from ship observations (Indian Daily Weather Report, Pune, India) within a radius of 2° around the three sediment trap locations. Wind-speed data were smoothed with a 5-point moving average. Peak fluxes occurring during the SW (June–September) and NE (December–February) monsoons show close similarity to wind-speed patterns and are related to high primary production resulting from wind-induced mixed layer deepening and associated nutrient injection in the euphotic zone[8,9], and is best established in the central Arabian Sea (see Fig. 3). The peak fluxes in the western Arabian Sea during July–August and between August–October in the eastern Arabian Sea also have components derived from nutrient advection[16] and lateral transport of material from the coastal upwelling centres. In the eastern Arabian Sea strong stratification resulting from the inflow of low-salinity water from the eastern tropical Indian Ocean during the NE monsoon leads to low productivity[13] reflected in low particle fluxes.

Further information on factors controlling the observed fluxes comes from the component fluxes (Table 1). Carbonates dominate the component fluxes and are present mainly in the form of coccolithophorids with a certain amount of foraminifera. Organic carbon and nitrogen fluxes are similar to those reported from other oceanic areas[15]. Major differences between sites were observed in the opal and lithogenic fluxes.

In the central and eastern Arabian Sea sites, opal accounts for 12% and 13% of the total flux. In the western Arabian Sea, opal contributed up to 22% of the total annual flux and accounted for as much as 40% during the peak fluxes in July and August, mostly in the form of the diatom *Rhizosolenia*, a major upwelling species. During the summer monsoon of 1986, waters from the Somali-Arabian upwelling centres have been shown to be advected up to 60° E (ref. 16). Peak fluxes at this site located more than 400 km from the continental margin thus have a component derived from nutrient-rich upwelled water transported offshore.

High lithogenic fluxes are associated with the south-west monsoon (June to September) and their contribution to total fluxes increases from the western (9%) to the eastern (25%) Arabian Sea site (Table 1). Eolian input to the Arabian Sea is restricted by the Somali Jet to the northwestern parts, and may constitute an important source of lithogenic particles at the western Arabian Sea site (ref. 17; F. Sirocco and M. Sarnthein, manuscript in preparation). In the northeastern and central parts of the Arabian Sea the chief suppliers of lithogenic material are the rivers Indus, Narmada and Tapti. More than 80% of their annual suspended-matter discharge occurs during the south-west monsoon[18]. The simultaneous prevalence of clockwise surface currents in the Arabian Sea can divert lithogenic material to the eastern Arabian Sea, contributing to its relative enrichment. Sediment-trap studies in the outer shelf off Goa, India, have shown Indus-derived sediment to be a significant component during this period[19].

Our results show that the particle fluxes out of the surface layers in the Arabian Sea are primarily linked to changes in the prevailing meteorological and hydrographical conditions through biological processes occurring in the surface layers. Higher wind speeds promote biological productivity by (1) enhancing the introduction of essential trace elements associated with atmospheric dust fallout (for instance, iron[20]), and (2) the

TABLE 1 Component fluxes of the fraction <1 mm to the deep Arabian Sea. The data are given for the SW (June–September), NE (December–February) monsoons and for the periods in between

Site	Components <1 mm	NE–SW g m^{-2}	%	SW Monsoon g m^{-2}	%	SW–NE g m^{-2}	%	NE monsoon g m^{-2}	%	Total g m^{-2}	%
Western Arabian Sea	carbonate	1.17	54.2	12.10	51.4	2.13	73.2	3.60	68.1	19.00	56.00
	opal	0.12	5.6	6.08	25.8	0.30	10.3	0.78	14.7	7.28	21.5
	lithogenic	0.11	5.1	2.10	8.9	0.28	9.6	0.15	2.8	2.64	7.8
	C_{org}	0.16	7.4	1.18	5.0	0.14	4.8	0.32	6.0	1.80	5.3
	N	0.02	0.9	0.14	0.6	0.02	0.7	0.04	0.8	0.22	0.6
	Total flux	2.16	6.4	23.56	69.5	2.91	8.6	5.29	15.6	33.92	
Central Arabian Sea	carbonate	0.49	57.6	9.31	66.4	2.15	66.8	5.55	66.4	17.50	66.2
	opal	0.06	7.1	1.51	10.8	0.35	10.9	1.16	13.9	3.08	11.6
	lithogenic	0.07	8.2	1.84	13.1	0.35	10.9	0.79	9.5	3.05	11.5
	C_{org}	0.06	7.1	0.74	5.3	0.20	6.2	0.53	6.3	1.53	5.8
	N	0.01	1.2	0.09	0.6	0.02	0.6	0.07	0.8	0.19	0.7
	Total flux	0.85	3.2	14.02	53.0	3.22	12.2	8.36	31.6	26.45	
Eastern Arabian Sea	carbonate	0.80	43.2	7.27	49.5	3.40	54.4	0.41	51.3	11.88	50.4
	opal	0.30	16.2	1.81	12.3	0.79	12.6	0.23	28.8	3.13	13.3
	lithogenic	0.42	22.7	3.60	24.5	1.35	21.6	0.03	3.8	5.40	22.9
	C_{org}	0.18	9.7	1.00	6.8	0.33	5.3	0.05	6.3	1.56	6.6
	N	0.02	1.1	0.10	0.7	0.04	0.6	0.01	1.2	0.17	0.7
	Total flux	1.85	7.8	14.68	62.3	6.25	26.5	0.80	3.4	23.58	

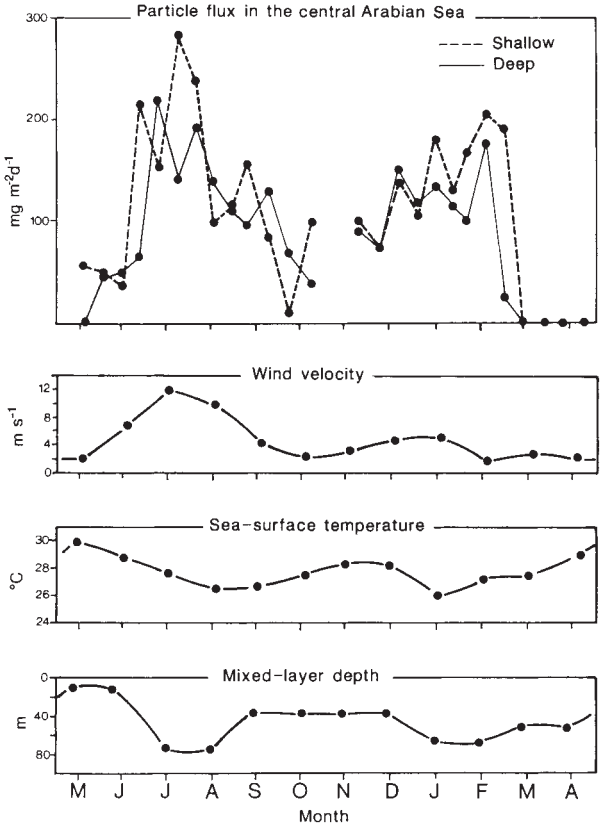

FIG. 3 Time-series (sampling intervals 12–13 days) of particle flux from two depths (shallow, 780 m; deep, 2,900 m) in the central Arabian Sea, and the general information on wind velocity[23], sea-surface temperature[1] and mixed layer depth[1]. Low sea-surface temperatures and a deeper mixed layer during these periods show that wind-induced mixing occurs which brings nutrient-rich water to the surface. The resultant high biological productivity leads to the observed flux pattern.

injection of new nutrients from deeper layers to the euphotic zone. There have been times in the recent geological past when wind speeds were higher than today's by a factor of 1.3 to 1.6, and the atmosphere had higher dust contents, for example during the glacial periods[21], which must have led to an increase in global ocean productivity. The subsequent removal of this new production to the deep ocean as deduced from our study could have contributed in part to low atmospheric CO_2 contents during the glacial periods[22]. □

Received 19 August 1988; accepted 3 March 1989.

1. Wyrtki, K. *Oceanographic Atlas of the International Indian Ocean Expedition* (National Science Foundation, Washington, 1971).
2. Bruce, J. G. *J. mar. Res.* **32,** 419–423 (1974).
3. Currie, R. I., Fisher, A. E. & Hargreaves, P. M. in *The Biology of the Indian Ocean* (eds Zeitschel, B. & Gerlach, S. A.) 37–52 (Springer, Berlin, 1973).
4. Sharma, G. S. *Indian J. Mar. Sci.* **7,** 209–218 (1976).
5. Honjo, S. & Doherty, K. W. *Deep Sea Res.* **35,** 133–149 (1988).
6. Honjo, S., Manganini, S. J. & Cole, J. J. *Deep Sea Res.* **29,** 609–625 (1982).
7. Michaelis, W. & Ittekkot, V. *Transport of Carbon and Minerals in World Rivers* Part 1 (ed Degens, E. T.) 233–243 (Mitt. Geol.-Pal. Inst., Univ. Hamburg, SCOPE/UNEP Sonderbd. 52, 1982).
8. Klein, P. & Coste, B. *Deep Sea Res.* **31,** 21–37 (1984).
9. Kiefer, D. A. & Kremer, J. N. *Deep Sea Res.* **28A,** 1087–1105 (1981).
10. Sastry, J. S. & Ramesh Babu, V. *Proc. Indian Acad. Sci. (Earth planet. Sci.)* **94,** 117–128 (1985).
11. Ryther, J. H. & Menzel, D. W. *Deep Sea Res.* **12,** 199–209 (1965).
12. Banse, K. *Deep Sea Res.* **34,** 713–723 (1987).
13. Banse, K. & McClain, C. R. *Mar. Ecol. Prog. Ser.* **34,** 201–211 (1986).
14. Qasim, S. Z. *Deep Sea Res.* **29,** 1041–1068 (1982).
15. Tsunogai, S. & Noriki, S. *Deep Sea Res.* **34,** 755–767 (1987).
16. Vinayachandra, P. N., Sadhuram, Y. & Ramesh Babu, V. *Tellus* (submitted).
17. Savoie, D. L., Prospero, J. M. & Nees, R. T. *J. geophys. Res.* **92,** 933–942 (1987).
18. Ittekkot, V. & Arain, R. *Geochim. cosmochim. Acta* **50,** 1643–1653 (1986).
19. Ramaswamy, V. in *Particle Flux in the Ocean* (eds Degens, E. T., Honjo, S. & Izdar, E.) 233–243 (Mirtt. Geol.-Pal. Inst., Univ. Hamburg, SCOPE/UNEP Sonderbd. 62, 1987).
20. Martin, J. H. & Fitzwater, S. E. *Nature* **331,** 341–343 (1988).
21. Petit, J. R., Briat, M. & Royer, A. *Nature* **293,** 391–394 (1981).
22. Barnola, J. M., Raynaud, D., Korotkevich, Y. S. & Lorius, C. *Nature* **329,** 408–414 (1987).
23. Ramage, G., Miller, F. R. & Jefferies, C. *International Indian Ocean Expedition Atlas 1: the surface climate of 1963 and 1964* (East West Center, Honolulu, 1969).

ACKNOWLEDGEMENTS. We thank R. Venkatesan, D. Gracias and P. Jöhrendt for technical assistance, and the officers and crew of the research vessels R/V *Sonne* and ORV *Sagar Kanya* for help in the deployment and recovery of the mooring systems. We also thank Dr J. Dymond for his review and comments. Financial support from the Federal German Ministry for Research and Technology, Bonn, and the Council of Scientific and Industrial Research, New Delhi, and the allotment of the ship time on ORV *Sagar Kanya* by the Department of Ocean Development (New Delhi) are gratefully acknowledged.

Barium content of benthic foraminifera controlled by bottom-water composition

D. Lea & E. Boyle

Department of Earth, Atmospheric and Planetary Sciences, Massachusetts Institute of Technology, Cambridge, Massachusetts 02139, USA

THE carbon isotope ratio ($\delta^{13}C$) and cadmium content (Cd/Ca) of benthic foraminifera shells have been used to reconstruct deep-water circulation patterns of the glacial oceans[1–7]. These tracers co-vary with phosphorus in the modern ocean because they are nearly quantitatively regenerated from sinking biological debris in the upper water column. Hence they can be used to reconstruct the distribution of labile nutrients in glacial water masses. Independent constraints on glacial deep-ocean circulation patterns could be provided by a tracer of the distribution of silica and alkalinity, the deeply regenerated constituents of planktonic hard parts. Barium shares key aspects of its behaviour with these refractory nutrients because it is removed from solution in surface waters and incorporated into sinking particles which slowly dissolve deep in the water column and in the sediments[8]. The fractionation of Ba between deep-water masses of the major ocean basins is largely controlled by thermohaline circulation patterns, so Ba conforms to different boundary conditions from Cd and $\delta^{13}C$. As Ba substitutes into trigonal carbonates[9], it is a potential palaeoceanographic tracer if the Ba content of foraminifera shells reflects ambient dissolved Ba concentrations. Here we present data from Recent core-top benthic foraminifera which indicate that the Ba content of some recent calcitic benthic foraminifera does co-vary with bottom-water Ba.

The distribution of barium, alkalinity and silica in the world's oceans was mapped extensively during the GEOSECS

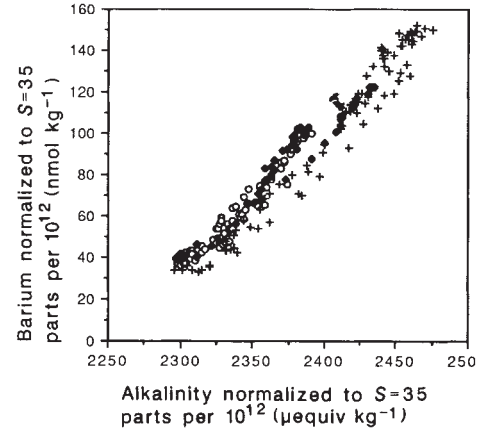

FIG. 1 Paired Ba and alkalinity data from ocean water samples analysed for the GEOSECS program[10–13]. Alkalinity and barium are normalized to a constant salinity of 35‰. Included are: Atlantic Ocean stations 29, 82 and 111 (circles); Pacific Ocean stations 204, 226, 312 and 322 (crosses); and Indian Ocean stations 429 and 452 (diamonds).